Revisiting the use of hyperdiffusivities in numerical dynamo models

Alexandre Fournier[1⋆] and Julien Aubert[2]

[1] Géomagnétisme, Institut de Physique du Globe de Paris, France, fournier@ipgp.fr
[2] Dynamique des Fluides Géologiques, Institut de Physique du Globe de Paris, France

http://avsgeomag.ipgp.fr

Introduction

The groundbreaking numerical dynamo models of Glatzmaier & Roberts (1995) and Kuang & Bloxham (1997) received some criticism due to their use of hyperdiffusivities, whereby small scale processes artificially experience much stronger dissipation than large scale processes. This stronger dissipation they chose was anisotropic, in that it was only effective in the horizontal direction (see the formula given in the methodology box).
Following the same choice as the studies mentioned above (which had most notably $l_0 = 0$), Grote et al. (2000) showed in a fully nonlinear context that the usage of hyperdiffusivities could lead to substantially different dynamics and magnetic field generation mechanisms.
Without questioning the physical relevance of this parameterization of subgrid scale processes, we wish here to revisit the use of hyperdiffusivities, on the account of the observation that today's models are run with a truncation at much larger spherical harmonic degree than early models. Consequently, they do not require hyperdiffusivities to kick in at the largest scales (l_0 can be set to several tens). An exploration of those regions of parameter space less accessible to numerical models could therefore benefit from their use, provided they do not alter noticeably the largest scales of the dynamo (which are the ones expressing themselves in the record of the geomagnetic secular variation). We thus present here a comparison of the statistics of a reference direct numerical simulation with the statistics obtained via several hyperdiffusive simulations.

The model

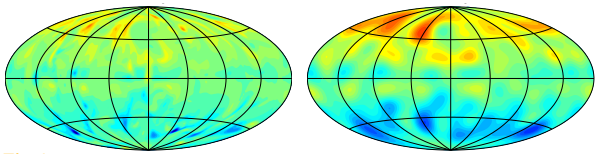

Fig. 1 A snapshot of the radial component of the field generated by the direct numerical simulation used for reference. Left: CMB field (full spectrum). Right: CMB field truncated at $l = 13$

Following the implementation of Dormy et al. (1998); Aubert et al. (2008), we solve for the conservation of mass, momentum, and energy of a convecting Boussinesq fluid in rapid rotation, in addition to the induction equation. We use the codensity formalism of Braginsky & Roberts (1995).

- Boundary conditions: flow: no-slip; field: insulating boundary condition at ICB and CMB; codensity: F_i (F_o) imposed at ICB (CMB).
- Purely chemical driving $f_i = \frac{F_i}{F_i + F_o} = 100\%$
- Input parameters
  $\mathrm{E} = 10^{-4}, \quad \mathrm{Pr} = 1, \quad \mathrm{Pm} = 1, \quad \mathrm{Ra} = \frac{g_o F}{4\pi\rho\nu\kappa\Omega} = 14,000$
  $\left(\mathrm{Ra}_\Omega = \text{this Ra} \times \mathrm{E}^2\mathrm{Pr}^{-1} = 1.4\,10^{-5}\right)$
- Output parameters $\mathrm{Re} = \mathrm{Rm} = 240$
  Scales : $\bar{l}$ (flow) $\sim 13 - 15$, $\bar{l}$ (field) $\sim 14 - 18$, $\bar{m}$ (flow) $\sim 6 - 7$, $\bar{m}$ (field) $\sim 6 - 7$.

Methodology

Following e.g. Glatzmaier & Roberts (1996), we parameterize eddy viscosities using the generic formula

$$\begin{aligned} \nu(l) &= \nu_0 \text{ if } l \le l_0, \\ \nu(l) &= \nu_0 \left[1 + a\,(l - l_0)^n\right] \text{ if } l > l_0, \end{aligned}$$

in which l is the spherical harmonic degree, ν_0 is a reference value, l_0 is the degree above which hyperdiffusivities start operating, and a and n are real numbers.

CASE	horizontal truncation	l_0	a	n
A (ref)	133	N/A	N/A	N/A
B	44	34	0.1	3
C	64	34	0.1	2
D	64	50	0.1	3
E	85	50	0.1	2
F	85	65	0.1	3

Tab. 1 List of cases considered in this study.

The number of radial levels is the same for each case (192).

- Each case (see Tab. 1) was integrated for 1.5 magnetic diffusive time τ_d
- Each model trajectory was sampled uniformly in time every $0.002\ \tau_\mathrm{d}$; this generated $N_e = 750$ samples

Time averaged kinetic and magnetic spectra

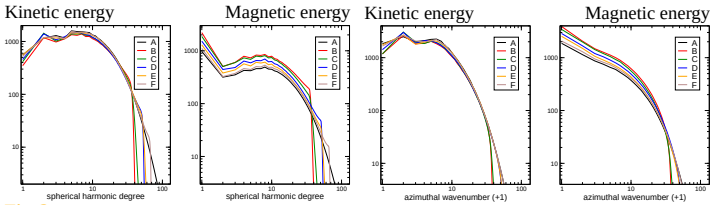

Fig. 2 Time averaged kinetic and magnetic spectra. From left to right: kinetic spectra, magnetic spectra (as a function of spherical harmonic degree l), kinetic spectra, magnetic spectra (against azimuthal wavenumber $m + 1$. Letters: cases as listed in Tab. 1.

The abrupt change of slope in the l-time averaged spectra points to the impact of hyperdiffusivities above the cutoff scale l_0; this impact is smoothed in the m spectra. In addition, we observe from Fig. 2. that above l_0, the kinetic spectra are less affected than the magnetic spectra by the truncation. We note that case F is remarkably similar to the reference DNS (case A).

Second-order statistics

We show in Fig. 4 part of the second-order statistics that would feed a data assimilation scheme based on these numerical models (Aubert & Fournier, 2011). As noticed in Aubert & Fournier (2011), the covariances between the surface field and the flow at mid-depth are mostly to be found between coefficients sharing the same m; these reflect the importance of convective columns in the dynamics. For practical purposes, we note that all cases lead essentially to the same structure for covariances.

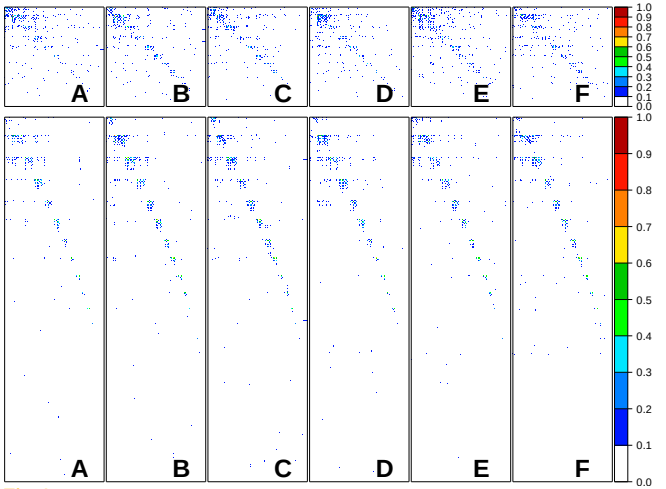

Fig. 4 Sub-blocks of the initial covariance matrix that would enter a data assimilation scheme based on the numerical models considered here (Aubert & Fournier, 2011). Top row: normalized covariance of the surface poloidal magnetic harmonic coefficients with the poloidal magnetic harmonic coefficients at mid-depth. Horizontal truncation at $l = 15$. Bottom row: normalized covariance of the surface poloidal magnetic harmonic coefficients with the poloidal velocity harmonic coefficients at mid-depth. Horizontal truncation set at $l = 15$ for the field and $l = 30$ for the flow.

Secular variation time scale

In view of using numerical dynamo models for the assimilation of geomagnetic observations (Fournier et al., 2010, 2011; Aubert & Fournier, 2011), the secular variation time scale τ_SV provides a convenient and sensible way of rescaling the time axis of 3D simulations (Lhuillier et al., 2011a).
The non-dipole SV time scales τ_l are modelled by an inverse linear law of the form

$$\tau_l = \frac{\tau_\mathrm{SV}}{l}.$$

(Christensen & Tilgner, 2004). Fig. 3 displays the secular variation time scales computed for all the cases considered here. All cases yield the same fit by an inverse linear law (black line), indicating that they would lead to the same rescaling of the time axis.

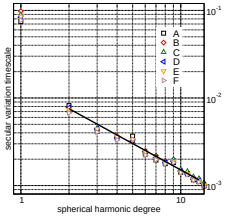

Fig. 3 Secular variation time scales τ_l as a function of spherical harmonic degree l, for spherical harmonic degrees comprised between 1 and 13. Black line: fit obtained using an inverse linear law, for the non-dipole SV. Letters refer to cases as listed in Tab. 1.

Summary

- A careful use of hyperdiffusivities above some well-chosen cut-off scale does not alter the first and second order statistics of numerical dynamo simulations
- This cutoff scale has to be chosen in the tail of the kinetic and magnetic spectra
- The use of hyperdiffusivities can allow for a significant reduction in cpu time when exploring the parameter space
- This reduction is likely to become even more pronounced as we want to approach geophysical conditions

References

Aubert, J. & Fournier, A., 2011. Inferring internal properties of Earth's core dynamics and their evolution from surface observations and a numerical geodynamo model, *Nonlinear Processes In Geophysics*, **18**(5), 657–674.

Aubert, J., Aurnou, J., & Wicht, J., 2008. The magnetic structure of convection-driven numerical dynamos, *Geophysical Journal International*, **172**(3), 945–956.

Braginsky, S. I. & Roberts, P. H., 1995. Equations governing convection in Earth's core and the geodynamo, *Geophysical & Astrophysical Fluid Dynamics*, **79**(1), 1–97.

Christensen, U. R. & Tilgner, A., 2004. Power requirement of the geodynamo from ohmic losses in numerical and laboratory dynamos, *Nature*, **429**(6988), 169–171.

Dormy, E., Cardin, P., & Jault, D., 1998. MHD flow in a slightly differentially rotating spherical shell, with conducting inner core, in a dipolar magnetic field, *Earth and Planetary Science Letters*, **160**(1-2), 15–30.

Fournier, A., Hulot, G., Jault, D., Kuang, W., Tangborn, A., Gillet, N., Canet, E., Aubert, J., & Lhuillier, F., 2010. An introduction to data assimilation and predictability in geomagnetism, *Space Science Reviews*, pp. 1–45, 10.1007/s11214-010-9669-4.

Fournier, A., Aubert, J., & Thébault, E., 2011. Inference on core surface flow from observations and 3-D dynamo modelling, *Geophysical Journal International*, **186**(1), 118–136.

Glatzmaier, G. A. & Roberts, P. H., 1995. A three-dimensional convective dynamo solution with rotating and finitely conducting inner core and mantle, *Physics of the Earth and Planetary Interiors*, **91**(1), 63–75.

Glatzmaier, G. A. & Roberts, P. H., 1996. An anelastic evolutionary geodynamo simulation driven by compositional and thermal convection, *Physica D: Nonlinear Phenomena*, **97**(1-3), 81–94.

Grote, E., Busse, F. H., & Tilgner, A., 2000. Effects of hyperdiffusivities on dynamo simulations, *Geophysical Research Letters*, **27**(13), 2001–2004.

Kuang, W. & Bloxham, J., 1997. An Earth-like numerical dynamo model, *Nature*, **389**(6649), 371–374.

Lhuillier, F., Fournier, A., Hulot, G., & Aubert, J., 2011a. The geomagnetic secular-variation timescale in observations and numerical dynamo models, *Geophysical Research Letters*, **38**, L09306.